Time-Resolved Quantum Dynamics of Double Ionization in Strong Laser Fields

Jakub S. Prauzner-Bechcicki,[1] Krzysztof Sacha,[1] Bruno Eckhardt,[2] and Jakub Zakrzewski[1]

[1]*Instytut Fizyki Mariana Smoluchowskiego and Mark Kac Complex Systems Research Center, Uniwersytet Jagielloński, Reymonta 4, 30-059 Kraków, Poland*

[2]*Fachbereich Physik, Philipps-Universität Marburg, D-35032 Marburg, Germany*

(Received 30 June 2006; published 15 May 2007)

Quantum calculations of a (1 + 1)-dimensional model for double ionization in strong laser fields are used to trace the time evolution from the ground state through ionization and rescattering to the two-electron escape. The subspace of symmetric escape, a prime characteristic of nonsequential double ionization, remains accessible by a judicious choice of 1D coordinates for the electrons. The time-resolved ionization fluxes show the onset of single and double ionization, the sequence of events during the pulse, and the influences of pulse duration and reveal the relative importance of sequential and nonsequential double ionization, even when ionization takes place during the same field cycle.

DOI: 10.1103/PhysRevLett.98.203002 PACS numbers: 32.80.Rm, 02.60.Cb, 03.65.−w, 32.80.Fb

Double ionization in intense laser fields has been challenging because of a yield much higher than derived from independent electron calculations, thus demonstrating the significance of electron interactions (see [1], and references therein). High resolution experiments revealed that the two outgoing electrons preferably leave the atom side by side, with the same parallel momenta [1,2]. The theoretical understanding and interpretation of this process is still far from being complete. The most accurate representations of the process, i.e., the exact solution of the time-dependent Schrödinger equation for two electrons in a laser field [3] or S-matrix calculations [4], are computationally demanding and still do not fully represent the experiments. Low-dimensional models frequently sacrifice the experimentally dominant subspace of symmetric escape by restricting the electrons to move along a common line (aligned-electron models) [5,6] or introduce other correlations, as in Ref. [7], where the motion of the electron center of mass is restricted to be along the field polarization axis. The (1 + 1)-dimensional model we present here removes these drawbacks and allows for efficient calculations which give time- and momentum-resolved insights into the dynamics of the process, from the turn-on of the field to the final escape of the electrons. While we concentrate here on double ionization of atoms in sinusoidal pulses, the construction of the reduced dimensionality model as well as the dynamical approach are quite general and can be applied to different pulses and in different situations dealing with the interaction of strong external fields with atoms or molecules.

The model is motivated by the rescattering scenario [8]. While most electrons leave the atom directly and contribute to the single ionization channel, some have their paths reversed by the field and return to the core. The acceleration by the field brings in enough energy so that, when this energy is shared with another electron close to the nucleus, each has enough energy to ionize. During the collision with the other electron, a short-lived compound state is formed which then decays into different possible channels: double ionization, single ionization, or a repetition of the rescattering cycle. Starting from this intermediate state, a classical analysis easily yields possible pathways to ionization [9]. The classical model of nonsequential double ionization (NSDI) suggests that the electrons may escape simultaneously if they pass sufficiently close to a saddle that forms in the symmetric subspace in the presence of the electric field. As the field phase changes, the saddle for this correlated electron escape moves along lines that keep a constant angle with respect to the polarization axis.

The observation that the saddles move along lines through the origin suggests a model where each electron is confined to move along this reaction coordinate [10]. This is the main difference between our model and the aligned-electron models, where a symmetric motion of the electrons is not possible because it is blocked by Coulomb repulsion between the electrons. With the present model, we are able to reproduce tunneling and rescattering processes and single and sequential double ionizations and to correctly mimic the possible contributions to correlated electron escape at all energies. Moreover, because of the restriction to 1 + 1 degrees of freedom, we can integrate the model with standard methods.

Taking into account that the lines form an angle of $\pi/6$ with the field axis [9], the restricted classical Hamiltonian for the two electrons in the linearly polarized laser field is given by (in atomic units) [10]

$$H = \sum_{i=1}^{2}\left(\frac{p_i^2}{2} - \frac{2}{|r_i|} + \frac{F(t)\sqrt{3}}{2} r_i\right) + \frac{1}{\sqrt{(r_1 - r_2)^2 + r_1 r_2}}, \tag{1}$$

where r_i are the electron coordinates along the saddle lines. The electric field is $F(t) = Ff(t)\sin(\omega t + \phi)$, with amplitude F, envelope $f(t)$, frequency ω (here $\omega = 0.06$ a.u.), and phase ϕ. For a fixed time and field $F(t)$, the potential energy (1) has a saddle located in the invariant sym-

metric subspace $r_1 = r_2$ and $p_1 = p_2$ at $|r_1| = |r_2| = 3^{1/4}/\sqrt{|F(t)|}$ of energy $V_s(t) = -3^{3/4}2\sqrt{|F(t)|}$ [11]. If the electrons pass close to this saddle and sufficiently close to the symmetric subspace, they can leave the atom simultaneously. The saddle defines the bottleneck for simultaneous escape. Once the electrons are outside the barrier, they are accelerated by the field and escape. Any asymmetry of electron motion around the saddle can be amplified by the field. Thus, even if they escape simultaneously, their final momenta can be quite different (see Ref. [10] for examples of classical trajectories in a static field). In this Letter, we analyze the quantum dynamics of this model by solving the time-dependent Schrödinger equation numerically by a Fourier method. The Coulomb singularities in the potential in (1) are smoothed by the substitution $1/x \rightarrow 1/\sqrt{x^2 + e}$, with $e = 0.6$, which leads to a ground state energy of the unperturbed atom of $E_g = -2.83$.

For the analysis of the outgoing electrons, we follow Ref. [3] and define regions in the configuration space that correspond to the neutral atom (A), the singly ionized atom (S_i), and the doubly ionized atom (D_i) (see Fig. 1). These definitions are suggested by practical considerations and correspond effectively to a truncation of the long range effects of the Coulomb potential at these distances. The regions allow us to distinguish between the sequential and the nonsequential (simultaneous) double ionization by calculating the probability fluxes between the appropriate regions: (i) The population of the singly ionized states at a time t is obtained from the time integration of the fluxes from A to S_i minus the fluxes from S_i to D_i; (ii) the population of NSDI states is obtained from the time integration of the fluxes from A to D_1 and from A to D_3; (iii) integration of the fluxes from S_i to D_j gives a measure of sequential double ionization (SDI) processes. The fluxes from A to D_2 and from A to D_4 correspond to anticorrelated double ionization: They give negligible contributions to the double ionization process and will not be considered further here. Note that the definition of the fluxes allows us to distinguish two contributions to the instantaneous double ionization yield: Electrons may pass directly from region A to D_1, say, or they may first cross over to S_1 and then to D_1. The essential difference between the two paths is that in the first case electron interactions are significant, whereas in the second case the electrons remain sufficiently far apart that their interactions are negligible. We will limit the use of the term NSDI to the first situation, where electron-electron interactions remain relevant also in the outgoing channel. Other multiple ionization processes, such as recollision excitation of the second electron (RESI) as discussed in Ref. [12] are collected in the SDI channel.

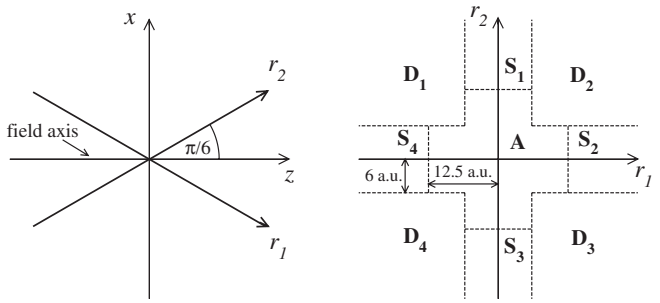

FIG. 1. Geometry of the model. The left frame shows the lines along which the electrons can move. The right frame shows the division of the configuration space r_1-r_2 into domains assigned to the neutral atom A, singly charged ions S_i, and doubly charged ions D_i, each with indices $1, \ldots, 4$. The polarization axis points along z.

As a first result, we show the ionization yields for the different subspaces in Fig. 2. They are calculated from the fluxes as described in the preceding section. For intermediate fields, the NSDI and SDI signals are about equal, but for higher fields SDI rises sharply, forming the well-known knee: In hindsight, it is clear that only the sequential double ionization can show the knee, as it derives from the strong increase of independent electron ionization at high fields. The NSDI signal, on the other hand, seems to saturate for field amplitudes above about 0.25 a.u.

The time ordering of the process, resolved into the different fluxes, is shown in Fig. 3 for a field strength of $F = 0.16$, below the knee. Up to the fourth extremum, the field is not strong enough to ionize any electrons. Shortly thereafter, singly charged ions appear but no doubly charged ones. Immediately after the fifth extremum, a strong single ionization is observed as well as a first double ionization signal. Note that the maximum of double ionization occurs shortly after the extremal field strength, at about the same time as the maximum in the single ionization signal. This shows that a significant fraction of the double ionization events occur when the field is still on.

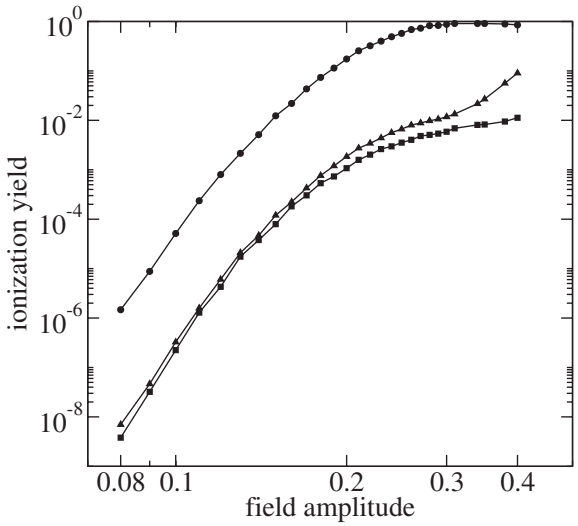

FIG. 2. Yields for single ionization (circles), sequential double (triangles) ionization, and nonsequential double (squares) ionization as a function of the field amplitude. The data are obtained for the initial phase of the field $\phi = 0$ and the pulse envelope $f(t) = \sin^2(\pi t/T)$, where pulse duration T equals 5 field cycles.

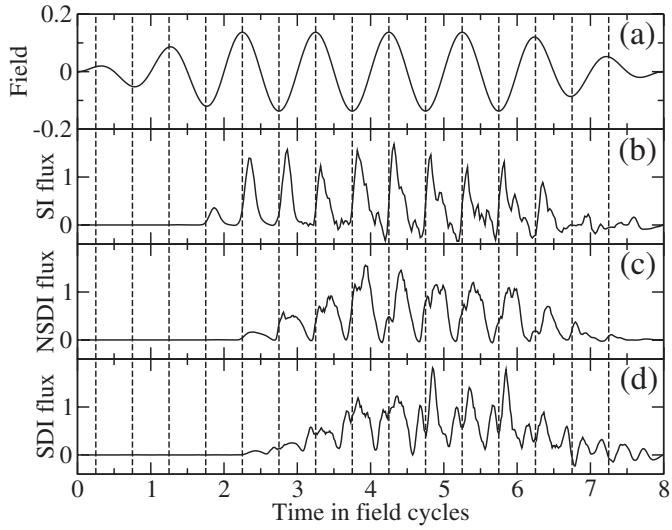

FIG. 3. Probability fluxes (in arbitrary units) as a function of time. (a) shows the field strength for $F = 0.16$. (b) shows the flux related to the single ionization, and (c) and (d) show the nonsequential and sequential double ionization yields, respectively. The field has an initial phase $\phi = 0$, a duration of 8 cycles, and is switched on and off linearly over 2 cycles.

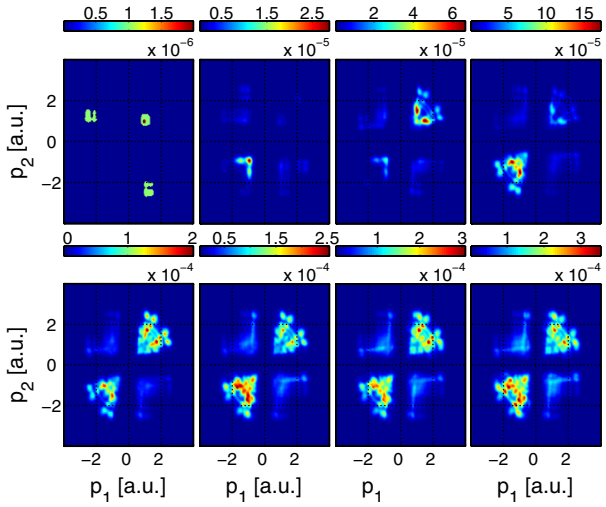

FIG. 4 (color online). Time-resolved electron momentum distributions corresponding to the field parameters in Fig. 3. The times equal the extrema of the field strengths, indicated by the dashed lines in Fig. 3, starting with the one at $t = 3.75$ cycles (top left) and ending with 7.25 (bottom right).

The momentum distributions of the outgoing electrons are obtained following the method proposed in Ref. [6], where the wave function is propagated with all interactions in a region of width 400 a.u. $\times$ 400 a.u. Outside this domain, the wave function is transformed to the momentum space where time evolution (with neglected Coulomb potentials and in the velocity gauge) becomes simply a multiplication by a time-dependent phase. Fourier transforms of the parts of the wave function in the regions $|r_1|, |r_2| > 200$ a.u. then give the momentum distributions in Fig. 4.

The panels in Fig. 4 are calculated for the same parameters as for Fig. 3 and give the momentum distribution at successive extrema of the field. The sequence starts with the extremum at 3.75 cycles, as there is no noticeable wave function amplitude in the range $|r_1|, |r_2| > 200$ a.u. for earlier extrema. The wave function that gives rise to the NSDI near times of $t = 2.25$ oscillates with the field and extends into this space region only about 1.5 cycles later. With this delay taken into account, the first signals in the NSDI sector in Fig. 4 correspond to the first signals in Fig. 3. The momentum distributions in the first four panels in Fig. 4 start out very much concentrated along the diagonal $p_1 = p_2$. This confirms that the bottleneck for double ionization is the saddle configurations in the symmetric subspace, described in Ref. [9]. The distributions also show that, during the first few cycles, there is a strong correlation between the direction of the extremum of the field and the momenta of the ejected electrons. Later on, also the other quadrants are populated, with the main contribution perhaps coming from accumulated rescattering excitations (RESI) [12].

After a few cycles, the different ionization signals in Fig. 3 and the momentum distributions in Fig. 4 experience significant spreading and distortion. They then no longer reflect the sequence of extrema and rescattering events, and the temporal relation between the individual processes gets blurred. Moreover, as time goes on, less correlated and purely sequential processes become more important. This suggests that the structure of the process can best be resolved with short pulses, say, up to 3 field cycles. This is shorter than the pulses used so far [2] but within experimental reach [13].

The time ordering of the process and, in particular, the presence of the field when the electrons return to the nucleus in the rescattering event can also be understood from the classical dynamics, as in Ref. [8], if the Coulomb field is taken into account. To this end, we show in Fig. 5 the results from a classical trajectory calculation. As in Ref. [8], we assume that an electron that tunnels out is released with zero momentum at the other side of the potential barrier. It is then integrated classically until it returns to the atom. Since the process involves motion of a single electron along the field axis, we can take a 1D Hamiltonian $H_1 = p^2/2 - 1/\sqrt{r^2 + e} + r(\sqrt{3}/2)F\sin(\omega t)$. The electron that tunnels through the Stark barrier starts with an energy -0.83 a.u., equal to the energy difference between the ground state of a He atom and a He^+ ion in our model [8]. If the field is weak, the electron starts far from the core and can acquire considerable energy while the field brings it back. However, such processes are very unlikely since the tunneling probability is negligible. The relevant energy parameter when the electron returns to the nucleus is the difference between energy of the two-electron system $E(t_r)$ and the potential energy of the saddle $V_s(t_r)$ [9,10], defining $\Delta E = E(t_r) - V_s(t_r)$. The data collected in Fig. 5 (corresponding to $F = 0.16$) clearly show that most electrons return while the field is still on, in

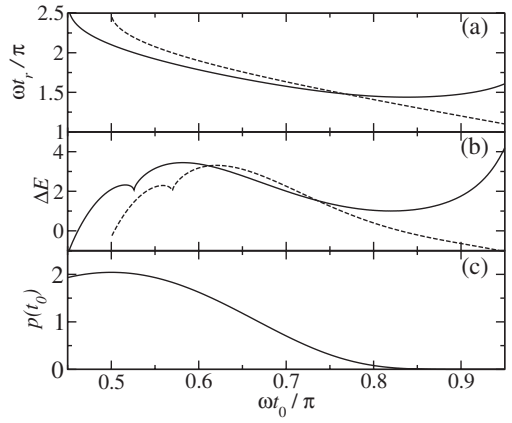

FIG. 5. Rescattering in a 1D model at $F = 0.16$. (a) shows the return time t_r, (b) the excess energy at the recollision moment t_r, and (c) the tunneling probability, obtained from a semiclassical estimate $\propto e^{-S}$, where S is the action of a tunneling trajectory, in unscaled units. The abscissa for all panels is the point in time where the electrons tunnel through the barrier (their initial energy is -0.83). Dashed lines in (a) and (b) show the results of the model with neglected Coulomb potential [1,8].

agreement with the sequence of events documented in Fig. 3. For smaller F, the range of positive excess energy shrinks and moves towards larger values of t_0, where the tunneling probability is negligible. This indicates that as F increases one cannot expect a sharp threshold behavior for the correlated simultaneous escape, since the contributions from the correlated events grow smoothly with field amplitude.

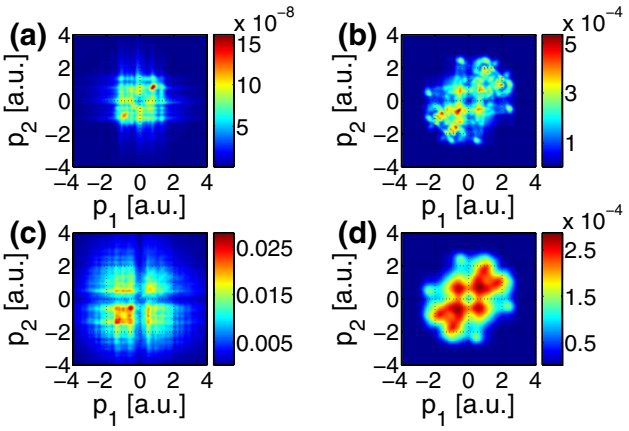

FIG. 6 (color online). Final electron momentum distributions for different field strengths. The pulse is 8 cycles long with a linear switch on and off over 2 cycles. The momentum distributions are averaged with a Gaussian of width 0.07 a.u. to model experimental resolution (and to remove finite size fluctuations from our numerical grid). The field phase is $\phi = 0$, and the amplitudes are (a) $F = 0.08$, (b) $F = 0.16$, and (c) $F = 0.4$. In order to show the effects of a varying phase and broader smoothing, (d) shows results for $F = 0.16$ but averaged over an undetermined phase ϕ and a wider Gaussian window of 0.2 a.u. The data are the Fourier transforms of the parts of the wave function (evolved one more cycle after the pulse is gone) in the regions $|r_1|, |r_2| > 100$ a.u.

Figure 6 shows results for an eight-cycle pulse and different field strengths. The figure can be compared with Fig. 1 of Ref. [6] obtained in the aligned-electron model, where, due to the overestimated Coulomb repulsion, the area around $p_1 = p_2$ is not populated. Here this region is accessible and provides information about the correlated electron escape. With increasing F, the double ionization signal increases, but above the knee ($F = 0.4$) the strong contributions in the second and fourth quadrants show the strong influence of SDI. The distributions for undetermined phase and wide averaging in Fig. 6(d) still show the strong concentration of the momentum near the diagonal, but the interference structures in the corresponding Fig. 6(b) are washed out. The investigation of these interference patterns is the subject of ongoing work.

We thank the Alexander von Humboldt Foundation, Deutsche Forschungsgmeinschaft, Marie Curie TOK COCOS project (MTKD-CT-2004-517186), and KBN through Grant No. PBZ-MIN-008/P03/2030 (J. Z.) and Polish Government scientific funds (KS:2005-2008, JPB:2005-2006) for support.

[1] A. Becker, R. Dörner, and R. Moshammer, J. Phys. B **38**, S753 (2005).
[2] T. Weber *et al.*, Nature (London) **405**, 658 (2000); B. Feuerstein *et al.*, Phys. Rev. Lett. **87**, 043003 (2001); R. Moshammer *et al.*, J. Phys. B **36**, L113 (2003).
[3] J. Parker *et al.*, J. Phys. B **29**, L33 (1996); D. Dundas *et al.*, J. Phys. B **32**, L231 (1999); J. Parker *et al.*, Phys. Rev. Lett. **96**, 133001 (2006).
[4] A. Becker and F. H. M. Faisal, Phys. Rev. Lett. **84**, 3546 (2000); R. Kopold *et al.*, Phys. Rev. Lett. **85**, 3781 (2000).
[5] R. Grobe and J. H. Eberly, Phys. Rev. A **48**, 4664 (1993); D. Bauer, Phys. Rev. A **56**, 3028 (1997); D. G. Lappas and R. van Leeuwen, J. Phys. B **31**, L249 (1998); W.-C. Liu *et al.*, Phys. Rev. Lett. **83**, 520 (1999); S. L. Haan *et al.*, Phys. Rev. A **66**, 061402(R) (2002).
[6] M. Lein, E. K. U. Gross, and V. Engel, Phys. Rev. Lett. **85**, 4707 (2000).
[7] C. Ruiz *et al.*, Phys. Rev. Lett. **96**, 053001 (2006).
[8] P. B. Corkum, Phys. Rev. Lett. **71**, 1994 (1993); K. C. Kulander, J. Cooper, and K. J. Schafer, Phys. Rev. A **51**, 561 (1995).
[9] K. Sacha and B. Eckhardt, Phys. Rev. A **63**, 043414 (2001); B. Eckhardt and K. Sacha, Europhys. Lett. **56**, 651 (2001).
[10] B. Eckhardt and K. Sacha, J. Phys. B **39**, 3865 (2006).
[11] Actually, in the restricted model considered here, the saddle is a maximum in the potential, but we will keep the name since it corresponds to a saddle in the full 3D situation.
[12] A. Rudenko *et al.*, Phys. Rev. Lett. **93**, 253001 (2004).
[13] M. Nisoli *et al.*, Opt. Lett. **22**, 522 (1997).